Real-time extended depth of field microscopy

Edward J. Botcherby, Martin J. Booth, Rimas Juškaitis and Tony Wilson

Department of Engineering Science, University of Oxford, Parks Road, Oxford, OX1 3PJ, United Kingdom

tony.wilson@eng.ox.ac.uk

Abstract: We describe an optical microscope system whose focal setting can be changed quickly without moving the objective lens or specimen. Using this system, diffraction limited images can be acquired from a wide range of focal settings without introducing optical aberrations that degrade image quality. We combine this system with a real time Nipkow disc based confocal microscope so as to permit the acquisition of extended depth of field images directly in a single frame of the CCD camera. We also demonstrate a simple modification that enables extended depth of field images to be acquired from different angles of perspective, where the angle can be changed over a continuous range by the user in real-time.

OCIS codes: (180.6900) Three-dimensional microscopy.

References and links

1. T. Wilson and C. J. R. Sheppard, "Theory and Practice of Scanning Optical Microscopy," Academic Press, London, (1984).
2. M. A. A. Neil, R. Juškaitis, T. Wilson, Z. J. Laczik, and V. Sarafis, "Optimized pupil-plane filters for confocal microscope point-spread function engineering," Opt. Lett. **25,** 245–247 (2000).
3. E. Botcherby, R. Juškaitis, and T. Wilson, "Scanning two photon fluorescence microscopy with extended depth of field," Opt. Comm. **268,** 253–260 (2006).
4. N. George and W.Chi, "Extended depth of field using a logarithmic asphere," J. Opt. A: Pure Appl. Opt. **5,** S157–S163 (2003).
5. E. R. Dowski and W. T. Cathey, "Extended depth of field through wave-front coding," Appl. Opt. **34,** 1859–1866 (1995).
6. M. Born and E. Wolf, *Principles of Optics* (Pergamon Press, 6th edition, 1983).
7. E. Botcherby, R. Juškaitis, M. Booth, and T. Wilson, "Aberration-free optical refocusing in high numerical aperture microscopy," Opt. Lett. **32,** 2007–2009 (2007).
8. E. Botcherby, R. Juškaitis, M. Booth, and T. Wilson, "An optical technique for remote focusing in microscopy," Opt. Comm. **281,** 880–887 (2008).

1. Introduction

The unique optical sectioning property of the confocal microscope enables it to image efficiently only those regions of a volume object which lie close to the focal plane [1]. A full three dimensional representation can therefore be obtained by refocusing the microscope and imaging a series of closely spaced planes in the specimen. This data can then be processed and displayed in a number of different ways to reveal a wealth of information about the specimen.

A particularly simple way of processing this data is to sum the component images together to generate an extended depth of field (EDF) image, so that information from the whole range of

#101239 - $15.00 USD Received 8 Sep 2008; revised 20 Nov 2008; accepted 24 Nov 2008; published 17 Dec 2008

specimen depths is displayed simultaneously. In this way the whole specimen can be surveyed at a glance. In some cases it may be desirable to acquire a sequence of EDF images in quick succession to monitor the dynamic behaviour of a specimen. The speed at which EDF images can be acquired, however, is fundamentally limited by the speed at which the microscope can be refocused to acquire the image stacks. A number of methods have therefore been developed to generate EDF images in a single exposure, using pupil plane masks [2, 3, 4] and wavefront coding [5]. These methods manipulate the system point spread function so as to gather information from a range of specimen depths on a single image and hence circumvent the need to acquire an image sequence. It should be noted, however, that the extension in the depth of field is these cases is generally obtained by compromising the quality of the system transfer function in some way. In this paper we present a novel focusing method that permits high speed, EDF images to be acquired directly on a CCD camera without compromising the system transfer function.

2. Focusing in microscopy

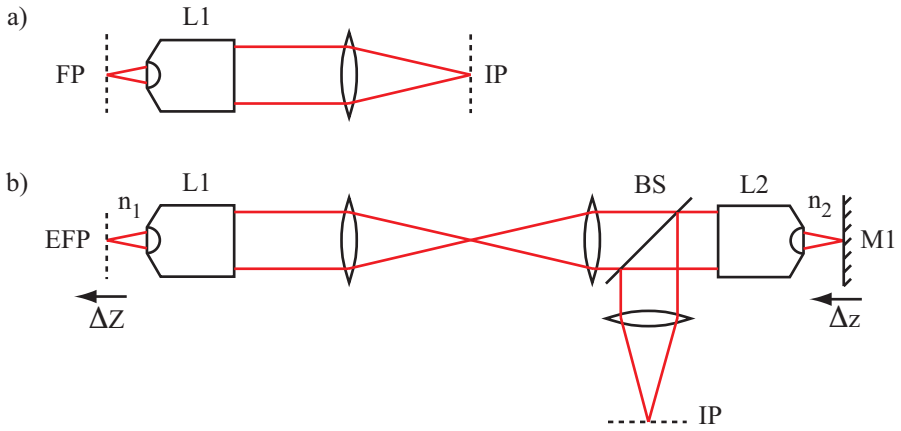

Fig. 1. (a) A standard microscope system and (b) a new architecture that permits remote focusing. In this arrangement the image plane is conjugate to an effective focal plane, whose axial position ΔZ depends on the position of mirror M. See main text for the definition of abbreviations.

Figure 1(a) shows the standard architecture on which most commercial microscope systems are built. This consists of a high numerical aperture (NA) objective lens (L1) and a low NA tube lens. L1 is usually designed to obey the sine condition [6] so that a diffraction limited image of the parts of the specimen lying in the focal plane (FP) appears in the image plane (IP) where the detector (camera) is placed. Unfortunately, for high NA systems, it is not possible to refocus this system remotely by simply shifting the detector position along the axis, as this process introduces spherical aberration that degrades image quality. The focal plane and image plane are therefore uniquely defined for each high NA lens. As a result, the only way to refocus this system, without introducing aberration, is to keep the image plane fixed and to change the physical distance between the objective lens and specimen mechanically. Unfortunately, the speed of this process is limited by the inertia of the objective lens and the specimen and is likely to be relatively slow. The specimen may also be subjected to agitations which affect the processes under observation. It is clear that all imaging techniques, and in particular confocal imaging, would benefit considerably from an alternative focusing method that does not require the objective lens or specimen to be moved physically, is fast enough not to limit the speed at

#101239 - $15.00 USD Received 8 Sep 2008; revised 20 Nov 2008; accepted 24 Nov 2008; published 17 Dec 2008

which images can be generated and does not introduce optical aberrations that degrade image quality while refocusing.

We have proposed a solution that circumvents these problems [7, 8]. Figure 1(b) shows the schematic layout of the basic concept, which comprises two high NA objective lenses, three achromatic doublet lenses, a mirror (M1) and a beam splitter (BS). The key feature of this arrangement is that the IP is now conjugated to an effective focal plane (EFP) in the specimen, whose axial position depends on the position of mirror M1 in the focal region of L2. As can be seen, the pupil planes of L1 and L2 are mapped onto one another with a $4f$ imaging system. If the magnification of this $4f$ system is chosen correctly, [8], then the aberrations introduced into the system by L2 directly cancel with those introduced by L1 when focusing onto different planes of the specimen. Hence, this system does not introduce any extra aberrations for different focal settings. Moving the mirror a distance Δz shifts the EFP by:

$$\Delta Z = \frac{2n_2}{n_1}\Delta z, \tag{1}$$

where n_1 and n_2 are the refractive indices of the immersion media for L1 and L2 respectively. We note that as M1 lies in the focal region of L2, it can be quite small. This, therefore, provides us with a much faster method of focusing than by moving the specimen or L1.

3. Nipkow disc confocal microscope

We combined this fast remote focusing architecture with a real-time Nipkow disc confocal microscope unit (CSU10, Yokogawa, Japan). The system, Fig. 2, also includes an extra mirror (M2) near the pupil plane of L1 (whose use we will discuss later). The pinhole array of the confocal microscope was placed in the image plane of the microscope. Illumination was provided by a diode pumped solid state laser (*Calypso*, Colbolt, Sweden) with a maximum available power of 50mW and wavelength of 491nm. The power and polarization of this laser could be adjusted externally with a neutral density filter set and a $\lambda/2$-plate respectively. A short focal length lens ($f = 16$mm) focused the laser light at the entrance aperture of the scanning unit so that the whole field of view in the specimen was illuminated. A dichroic beamsplitter with a cutoff wavelength of 493 nm and emission filter with a bandpass of 500-550nm were already embedded in the CSU10 for fluorescence imaging.

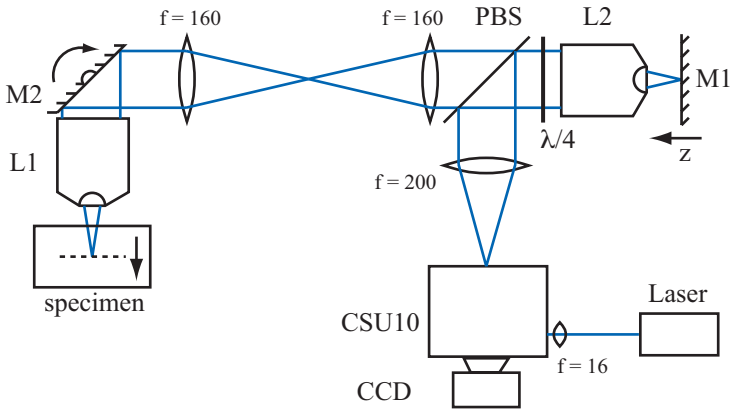

Fig. 2. Fluorescence confocal imaging system using a Nipkow disc. See main text for the definition of abbreviations.

#101239 - $15.00 USD Received 8 Sep 2008; revised 20 Nov 2008; accepted 24 Nov 2008; published 17 Dec 2008

A polarizing beamsplitter (PBS) and quarter-wave plate ($\lambda/4$) were used to direct all the illumination light through the system into the specimen and to ensure that a high proportion (50%) of the unpolarized fluorescence light passed back through the system into the CSU10. L1 and L2 were an Olympus 1.4 NA 60× oil immersion lens and an Olympus 0.95 NA 40× dry lens respectively. A dry lens was chosen for L2 to ensure that there was no mechanical interference between the scanning mirror and the objective. A coverglass of thickness 170μm was mounted onto the mirror since the objective L2 was coverglass corrected. A thin layer of oil was introduced between the mirror and coverglass to ensure good optical contact between these elements to minimize extraneous reflections that would otherwise result as the light passed between regions of different refractive index.

The 4f system mapping the pupil planes of the two objective lenses had unit magnification to ensure a complete cancellation of spherical aberration for different focal settings [8]. The lateral magnification of this system can be evaluated by considering mirror M1 in focus. In this situation, L2 does not affect the wavefronts in the pupil plane so the lateral magnification of the system is set by the combination of L1 and the 200mm doublet, which has a value of $60 \times \frac{200}{180} = 66.7\times$ because Olympus objectives are designed to operate with a tube lens of focal length 180mm. Images were acquired with a low noise, peltier cooled, CCD camera having 1344 x 1024 pixels (*ORCA-ER*, Hamamatsu, Japan). M1 was mounted on a piezo scanning stage (P-212.80, PI Instruments, Germany) so that its position along the axis could be controlled over a range of 100μm with a resolution of 0.1μm. The specimen was also mounted on a piezo scanning stage (P-611.3S NanoCube, PI Instruments, Germany), which provided a scanning range of 100μm along the axis.

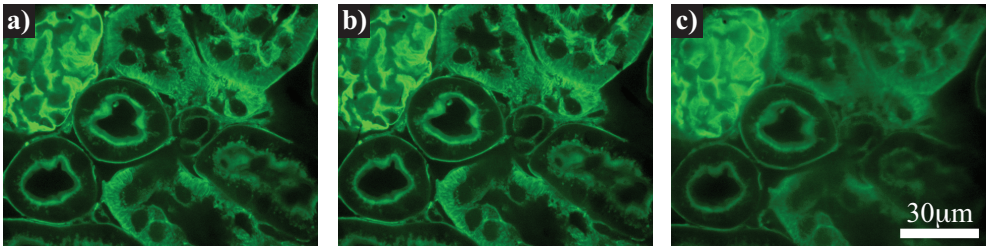

Fig. 3. Focusing 15μm below the surface of a mouse kidney specimen by (a) focusing with the new architecture, (b) moving the specimen itself and (c) by adjusting the image conjugate.

We began by demonstrating the effectiveness of the remote focusing method by recording images from a section of mouse kidney (FluoCells prepared slide #3, stained with Alexa Fluor 488, from Molecular Probes, Invitrogen). The surface of the specimen was brought into focus when M1 was in focus. The system was then refocused by scanning M1 along the axis towards L2 in order to image deeper planes. Figure 3(a) shows the image of the plane taken 15μm below the surface. We then returned the mirror M1 to the focal plane of L2 and focused the system by moving the specimen, as is usually done in commercial systems. We obtained the image of Fig. 3(b), again from a plane 15μm below the surface. In both images the fine detail of the specimen structure is clearly visible.

In order to demonstrate how spherical aberration affects image quality when focusing remotely with the standard microscope architecture we replaced L2 by a low NA (100mm focal length) achromatic doublet. M1 was placed in the focal position of this lens and the specimen was positioned so that its surface could be seen on the CCD. Focusing was then carried out by scanning M1 towards the lens using a manual stage. This was optically equivalent to placing the CSU10 pinhole array in the image plane of the standard microscope architecture (Fig. 1(a))

#101239 - $15.00 USD Received 8 Sep 2008; revised 20 Nov 2008; accepted 24 Nov 2008; published 17 Dec 2008

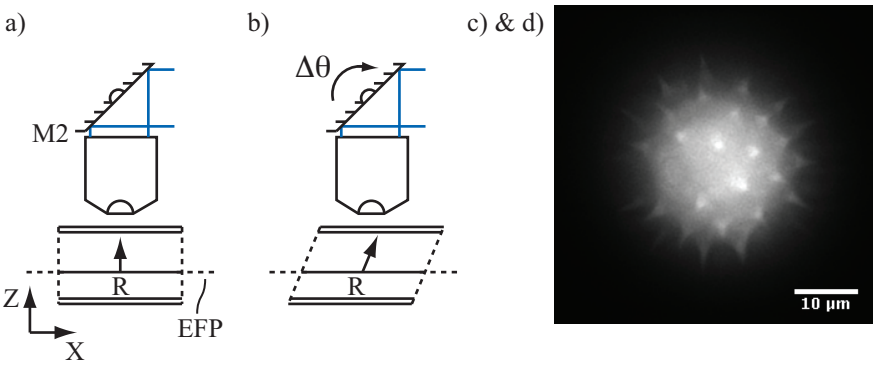

Fig. 4. (a) Trajectory of R during the acquisition of a single EDF image, (b) the trajectory of R when M2 is tilted in synchrony with the focusing action, (c) a single frame from an EDF movie of a pollen grain and (d) an EDF movie of a pollen grain where the perspective is changed by the user in real-time (Media 1).

and moving it towards the tube lens to image successively deeper planes of the sample. In Fig. 3(c) we show the same plane as before, 15μm below the surface, and draw attention to the degradation of image quality caused by spherical aberration that has been introduced by this method of focusing.

4. Extended depth of field imaging

As we have said, one way to generate an EDF image would be to record a series of sectioned images from different depths in the specimen and to sum these afterwards on a computer. However, the maximum rate at which EDF images can be generated by this method is N times slower than the frame-rate for acquiring each individual section, where N is the number of sectioned images required to make the EDF image. In the interest of speed we employed a different approach that permitted us to acquire EDF images directly in single frames of the CCD camera. At any instant in time, the CCD camera records information from a particular region (R) of the specimen that lies in the EFP. Refocusing the system changes the position of the EFP and therefore has the effect of sweeping R through the specimen axially. An EDF image can therefore be captured by simply sweeping R over a range of depths and integrating the response on the CCD (see Fig. 4(a)). Information from different layers of the specimen is summed directly on the CCD and no further processing is required. In addition, this procedure can be repeated a number of times in order to generate a real-time EDF movie.

Custom built software, written in Labview (National Instruments, USA) was used to control CCD integration while sweeping M1 through focus. The integration period was set to 100ms and M1 was swept over $\Delta z = 15.8\mu$m, which equated to sweeping R over an axial range of $\Delta Z = 20\mu$m in the specimen (from Eq. (1)). This particular choice of integration time was selected so as not to compromise the frame rate of the CCD camera. Figure 4(c) shows the EDF image of a pollen grain from a commercial sample (Carolina w.m. 30- 4264 (B690)). From this image it is possible to see that the specimen appears to be viewed from one particular direction, i.e. along the optic axis. This direction, of course, is defined by the trajectory of R as it sweeps through the specimen. In Fig. 4(b) we show how M2 can be used to modify this trajectory so that the EDF image appears to be viewed from a different angle of perspective. As M2 is sufficiently close to the objective lens it is reasonable to assume that it lies in the pupil plane. So a simple relationship exists between the lateral position, ΔX, of R and the angular tilt, θ, of

#101239 - $15.00 USD Received 8 Sep 2008; revised 20 Nov 2008; accepted 24 Nov 2008; published 17 Dec 2008

M2:

$$\Delta X = f \tan(\Delta\theta) \approx f\Delta\theta, \tag{2}$$

where f is the focal length of the objective lens. If we organize for M2 to tilt in synchrony with the focusing action of the microscope (mirror M1) then R can be forced to sweep out any desired linear trajectory in the specimen. The direction of this trajectory defines the angular perspective of the resulting EDF image and this can also be altered by changing the amplitude of the waveform driving M2. Using this method, therefore, it is possible to change the angular perspective of the EDF images acquired during the imaging process. To demonstrate this, we adapted our software to drive the tilting motion of M2. The movie in Fig. 4(d), shows the angle of perspective being changed continuously. From this, it is possible to determine without ambiguity which parts of the specimen lie in the foreground and background of the image.

5. Discussion and conclusion

We have shown that remote focusing can be readily applied to real-time Nipkow disc microscopy in order to acquire EDF images. In addition to this we have demonstrated how the apparent angle of perspective of these images can be altered in real-time by the user. This method of imaging is non-invasive as there are no mechanical movements produced near the specimen during imaging. Another benefit that can be gained from designing systems in this way is that of speed. As the focusing mirror (M1) can be made extremely small, it can be moved extremely quickly. As such, it is possible to use a resonance technique to permit focusing rates well into the kHz region. In this particular study, the maximum speed at which images could be acquired was limited by the CCD camera. However a faster camera could be employed to achieve faster imaging rates.

It is an interesting point to note that the resolution of this imaging system is determined by objective lens L1. At first glance, this might seem counterintuitive because L2 had a lower NA than L1 and would therefore appear to limit the resolution. This is not the case, however, because it is objective lens with the lowest *angular* aperture that determines the resolution in such systems [8]. As L1 had a larger angular aperture ($\alpha = \arcsin 1.4/1.518 = 67.3\,^{\circ}$) than L2 ($\alpha = \arcsin 0.95 = 71.8^{\circ}$), it is the NA of L1 that determined the resolution of the system.

Finally, we should like to point out that the method described here could be used to produce a stereo view of the specimen in real-time. This can be done by acquiring pairs of EDF images with differing angles of perspective, separated by approximately $12\,^{\circ}$. A stereo monitor could then be used to display these pairs of images in real-time so as to achieve a three dimensional perspective of the specimen. This would be particularly convenient as no additional visual aid would be needed to observe the stereo effect and hence this is likely to be a considerable advantage in biological studies, where it is important to monitor fast processes in three dimensions.

Acknowledgments

This work was supported by the Biotechnology and Biological Sciences Research Council (BBSRC). M. Booth is an Engineering and Physical Sciences Research Council (EPSRC) Advanced Research Fellow.

#101239 - $15.00 USD Received 8 Sep 2008; revised 20 Nov 2008; accepted 24 Nov 2008; published 17 Dec 2008